

The Modeling of Precipitation and Future Droughts of Mashhad Plain using Stochastic Time Series and Standardized Precipitation Index (SPI)

Salahi, B.^{1*}, Nohegar, A.² and Behrouzi, M.³

¹Department of Physical Geography, University of Mohaghegh Ardabili, Ardabil, Iran

²Faculty of Environment, University of Tehran, Tehran, Iran

³University of Malayer, Institute of grape, Malayer, Iran

Received 18 July 2016;

Revised 2 Sep. 2016;

Accepted 25 Sep. 2016

ABSTRACT: The purpose of this study is to model precipitation characteristics and simulation of drought using the Standardized Precipitation Index (SPI) during 2011-2020 in Mashhad station, Iran. To this end, first, the data related to the average of monthly precipitation in synoptic station of Mashhad (from 1951 to 2010) were obtained from the Meteorological Organization of Iran. Using the method proposed by Box-Jenkins, the monthly precipitation was modeled in 2011 to 2020, with respect to its preceding series trend. In addition, using SPI, climatic conditions in the upcoming years were investigated in terms of drought. The results indicated that the seasonal-multiplicative statistical model of SARIMA (2, 0, 1) (2, 1, 1)₁₂ is a good technique for fitting the precipitation data. Using this model, the pattern of monthly precipitation in Mashhad station from 2011 to 2020 was modeled. The results revealed that the average of monthly precipitation in the next 10 years will decrease about 26mm compared with the last 10 years (2001-2010). The correlation of precipitation in the upcoming 10 years compared with the previous 10 years is about 96%. The SPI suggested that in a 6-month timescale, in the upcoming 10 years, Mashhad station will face drought about 18%; in a 12-month timescale it would be about 17%.

Key words: Drought, Mashhad plain, Modeling, Precipitation, SPI, Time series

INTRODUCTION

Findings of atmospheric science researchers suggest that drastic changes in the behavior of climatic variables in the 21st century are signs of climate change (Dorand, 2014: 1). Precipitation along with temperature, as the most important and decisive climatic factors, are considered as suitable indicators for tracking climatic changes (Shirmohammadi, 2012: 2). In recent years, several important and major incidents have happened and caused a lot of damages to the lives of people. They have given rise to significant economic losses due to climate change (Khodaghohi et al., 2014: 3). Drought is one of the most chronic and economically devastating natural disasters. It is a natural hazard and disaster which emerges as a result of the lack of precipitation less than normal or expected amount (Hejazizadeh & Javizadeh, 2010: 17). Lower levels of rainfall and its extreme fluctuations lead to uncertainty in getting the required minimum amount of precipitation for agricultural purposes, human consumption, and providing water flow (ZandiLack et al., 2014: 3). Drought has often led to the creation of a lot of economic

*Corresponding author E-mail: bromand416@yahoo.com

changes, wars, famine, and migration. It seems that in the recent decades, the prevalence of this phenomenon in terms of intensity, duration, area of coverage, loss of life, economic losses, and long-term social consequences has been more than the other natural disasters (Shafiei et al., 2011: 4).

The Earth's climate is mainly characterized by two parameters of temperature and precipitation. Given the importance of drought and its impact on economic and social aspects of human beings, most recently many studies have been dedicated to this topic (Mohammadi, 2011: 5). Mishra and Deesa (2005) used linear statistical models of ARIMA and SARIMA to forecast droughts in the Kansabat river of India. They made predictions by the use of SPI data of this river, and then compared the results with the original data and came to the conclusion that there was not much difference between the predicted results and actual data. Cancelliere et al. (2007) predicted monthly drought through transfer functions of possibility and SPI with regard to the assumption of normality in monthly precipitation data.

Nirmala and Sundaram (2010) and Durdu (2010) used ARIMA and SARIMA models in their studies. Mohammadi (2011) showed that, in the time series of average station and cellular of Iran from 1964 to 2003, there was not any significant increase and decrease in the precipitation trend at the significance levels of 95 and 99%. However, the average of precipitation in stations of Iran has reduced about 0.64mm per year and the cellular average has reduced about 0.5 mm. Ozger et al. (2011), Mishra et al. (2011), Paulo et al. (2012), and Sheffield et al. (2012) have conducted similar studies in other regions. Han et al. (2013) used SPI to quantify the classification of drought in the Guanzhong Plain, China. They used autoregressive integrated moving average (ARIMA) models to fit and forecast the SPI series in this area. Chun et al. (2013) investigated the drought severity indices of six catchments for analyzing drought characteristics in the UK and modeled by ARIMA models and the generalized linear model. Shatanawi et al. (2013) monitored and forecast the drought in Jordan River Basin using ARIMA model and showed that this model could be used as a suitable forecasting tool for the future drought trends in this river basin. Meher and Jha (2013), Narayanan et al. (2013), and Abdul-Aziz et al. (2013) have also performed similar studies in other regions. Khodaghali et al. (2014) investigated future drought of Isfahan province by using ARIMA time series model. They showed that in some provinces' stations, the precipitation intensity would decrease until 2015 and the severity of the drought would increase. Ferrari et al. (2014), Yu et al. (2014), Bibi et al. (2014), Sopipan (2014), Wang et al. (2014), and Etuk and Mohamed (2014) investigated the pattern of drought indices in their studies. Mossad and Ali-Alazba (2015) used several ARIMA models for drought forecasting using the Standardized Precipitation Evapotranspiration Index in a hyper-arid climate. They showed that the ARIMA model (1, 1, 0) (2, 0, 1) could be considered as a general model for the Al Qassim region. Bazrafshan et al. (2015) used ARIMA and SARIMA model in forecasting the Standard Runoff Index (SRI) in Karkheh Basin and showed that the model accuracy was high in forecasting two months and one season of lead-time. Karavitis et al. (2015) showed that the seasonal Auto Regressive Integrated Moving Average Model (ARIMA) as well as SPI can evaluate short-term drought forecasting in Greece. Valipour (2015) integrated the ability of the SARIMA and ARIMA models for long-term runoff forecasting in the United States. He showed that there is a trend between annual runoff data in the United States every 20 years or almost a quarter century.

Tian et al. (2016) showed that the ARIMA models can forecast droughts and can also be applied to

forecast and evaluate them in the Guanzhong Plain. Bari et al. (2015) and Eni and Adeyeye (2015) also used ARIMA and SARIMA models in their researches. Tariq and Abbas (2016) showed that the SARIMA (0, 0, 0) x (0, 1, 1)₁₂ model is the most suitable model for simulating monthly rainfall over Nyala station in Sudan. Jayawardana et al. (2016) used SPI as the drought-monitoring tool with three different time scales in Sri Lanka. Perez et al. (2016) forecasted and monitored agricultural drought in the Philippines. Djerbouai and Souag-Gamane (2016) forecast drought using stochastic models in the Algerois basin in North Algeria. Alivia Chowdhury and Biswas (2016) and Matiur Rahman Molla et al. (2016) also used ARIMA and SARIMA models in order to model monthly precipitation in Krishnanagar Sub-Division (Nadia District, West Bengal) and Faridpur Region of Bangladesh, respectively. Mashhad plain, with annual rainfall of 251mm and the domination of arid and semi-arid climate, is in danger of drought conditions in nearly all years. For this reason, investigating the rainfall characteristics, the role and impact of drought in this part of Iran is essential. The purpose of this study is to model monthly precipitation in the upcoming years (2011- 2020) of Mashhad plain by using stochastic time series model and monitoring drought with various intensities using SPI.

MATERIALS & METHOD

Mashhad city, in terms of political division, is the administrative and political center of Khorasan-Razavi province. The city covers an area of 289 square kilometers with a height of 999.2 meters above the sea level (synoptic station). It is located in a geographical location within 16 minutes of 36 degrees in North and longitude of 59 degrees and 38 minutes in East along the catchment area of Kashf-Roud and between mountain ranges of Binaloud and Hezar-Masjed (Fig. 1). Mashhad, as the representative of Mashhad plain with the average annual precipitation of 251.5mm and the temperature of 14.3 °C in sampled period of 1951-2010, has a semi-arid climate. The maximum level of precipitation in part of Iran is in spring and the least amount is in summer. In order to achieve changes of precipitation and monitor drought in the upcoming years of Mashhad plain, monthly precipitation data from Mashhad synoptic station in a period of 60 years (1951-2010) were used. For the modeling of time series of monthly precipitation in Mashhad, the non-randomized and homogeneous quality of the monthly precipitation data was assessed through Ran test with a confidence level of 95% in the software environment of Minitab statistical analysis.

Some climatic incidents in successive observations and under specified conditions over time do not show

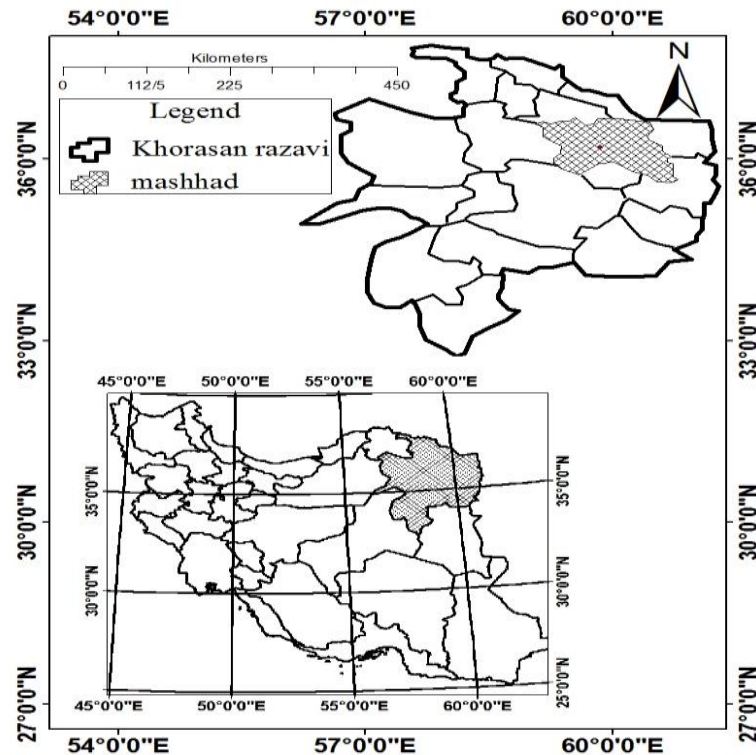


Fig. 1. Location of the city of Mashhad in Iran

the same results and it is possible that each time, they offer different conditions than the rest of the representations. Such phenomena, or similar phenomena, are called random processes (Asakare, 2007: 106). A stochastic process is a set of random variables which shows different values (observations) over time. For example, temperature, precipitation, pressure, relative humidity and the like are considered stochastic processes. Climatic events as random phenomena cannot be predicted precisely, but, through the constant observations, we get useful information which can be defined through possible rules. For example, it may be possible that a climatic process (e.g. $\{Z_t\}$) follows a particular statistical distribution or a certain behavioral model. One of the models suitable for fitting climatic processes is the ARIMA model. In this case, the random process $\{Z_t\}$ is called an ARIMA process with degrees of (p, d, q) and is written as z^H ARIMA (p, d, q) . Seasonal time series of Box-Jenkins model is form $(p, d, q) (P, D, Q)$ and in the formation, (P, D, Q) is the seasonality of model and the (p, d, q) is the non-seasonality of the model (Golabi et al, 2014:64). Seasonal time series model by Box-Jenkins SARIMA $(p, d, q) (P, D, Q)$ is written as equation (1):

$$p(B) P(BS) \nabla^d \nabla_{DS} x_t = q(B) (BS) z_t + 0 \quad (1)$$

which is well known as seasonal multiplicative ARIMA model and in that:

$$p(B) = 1 - 1B - 2B - \dots - PBP \quad (2)$$

Nonseasonality autoregressive operator of P order:

$$P(BS) = 1 - 1BS - 2B2S - \dots - PBPS \quad (3)$$

Seasonality autoregressive operator of p order:

$$q(B) = 1 - 1B - 2B^2 - \dots - qB^q \quad (4)$$

Nonseasonality moving average operator of q order:

$$(BS) = 1 - 1BS - 2B2S - \dots - BS \quad (5)$$

Seasonality moving average operator of Q order:

$$0 = \mu P(B) P(BS) \quad (6)$$

In the above equations, (B) , B & B are the, polynomials with P , p , q , Q orders, respectively. Coefficients of p , q are non-seasonality order and P , Q are seasonality order of autoregressive and moving average processes. In these equations, D and d show the simple and seasonality differencing, respectively. In this model, “ ds is the seasonality operator and Δds is the non-seasonal operator (Golabi et al., 2014: 64).

In these equations, $0, 1, \dots, Q, 1, \dots, q, 1, \dots, p, 1, \dots, p$ are unknown parameters of the model and must be estimated based on the sample data (Shabani et al., 2013: 898). Next, the method of time series and the general pattern of Box-Jenkins were employed. The main stages of construction in prediction model of Box-Jenkins include pattern recognition, pattern fitting, and investigating the

pattern relation (Dodange et al., 2012: 61). In the phase of pattern recognition, the first stage is drawing time series graphs. In this research, Minitab statistical software was used for diagramming. Series graph helps identify trends, stationary of variance, seasonality, and detection of outlier data (Ismaeilnejad, 2013: 131). In order to detect the presence of the trend (or its absence) in data, Mann-Kendall test was used.

Mann-Kendall test was originally offered by Mann (1945) and then was developed and expanded by Kendall (1975). This method is applied commonly and extensively in trend analysis of hydrological series and climatology (Alizadeh, 2015: 815). Among the advantages of this approach, we can refer to its suitability to use those time series that do not follow a specific statistical distribution. Minimal impressionability from limit values observed in some time series is another advantage of this method. The null hypothesis implies the randomness and lack of trends in data series, and accepting the hypothesis of the study (rejecting the null hypothesis) implies the existence of trends in data series (Shirmohammadi, 2012: 38). The stages of calculation in this test are as follows:
 - Comparison of each time series sentences p_1, p_2, \dots, p_n , with the next sentences. C_i calculation refers to the number of data after the i data, and should be larger than it. Having c_i for each element of time series till element $n-1$, total Series c_1, c_2, \dots, c_{n-1} or statistics rank of i is determined through equation (7):

$$= \sum_{i=1}^{n-1} c_i \quad (7)$$

The expected value ($E(\)$) and the variance ($V(\)$) are obtained through relations (8 and 9):

$$E(\) = n(n-1)(2n+5)/72 \quad (8)$$

$$v(\) = n(n-1)/4 \quad (9)$$

Mann-Kendall statistics are obtained from the equation (10) (Azarakhshi et al., 2013:3):

$$MK = T - E(\) / \sqrt{v(\)} \quad (10)$$

The null hypothesis (absence of trend) against the first hypothesis (existence of trend) is rejected when a confidence interval is established according to equation (11):

$$P=95\% \quad \Pr(|Z| < |KM|) > P \quad (11)$$

The next stage is the control of stationary time series. Time series is stable and stationary when characteristics such as mean and variance over time have fluctuations around a constant average (Ghahreman & Gharekhani, 2011: 78). In order to control stability in the mean and variance, the nonparametric

statistical quality control charts were used. If the series is non-stationary regarding the mean, differencing the series must be used (Golabi et al, 2014: 65). Differencing of time series is done through backward operator. B is backward operator which is defined as $BMXT = XT - M$. ∇ D is called non-seasonal operator from the order of d which is defined as $\nabla^d = (1-B)^d$. ∇^s D is called seasonal operator from D order and is defined as $\nabla^s = (1-BS)^D$ (Khazaei Moghani et al., 2014: 189). If series is non-stationary in variance, the best solution to make it stationary is to use Box-Cox transformations (Ismaeilnejad, 2013: 183). In this study, in order to detect non-stationary variance, Bartlets and Levenes tests were used. After explaining the stationary quality in variance and average and investigating trend in monthly precipitation data, time series seasonal pattern should also be removed. To this end, the series has been differenced with lag of 12 and its order is first order differencing, so seasonality series once is differenced with first order, and order of D in the final model series of SARIMA (p, d, q) (P, D, Q) S , will be one. Then, from the autocorrelation, functions chart (ACF), orders of Q and q were determined and based on partial autocorrelation chart (PACF), orders of P and p were determined. At the time of fitting the pattern, the unknown parameters of the model were estimated based on the method of least unconditioned squares. For measuring the suitability of the model, two complement methods were used: 1) The analysis of the residuals of the fitted model including the assumption of normality of residuals, independence of residuals and remaining stable the variance of residuals, and 2) A more comprehensive analysis. Finally, the best and the most appropriate statistical model for monthly precipitation data of Mashhad was selected and using the adjusted model, monthly precipitation data of Mashhad station were simulated and estimated for the next 10 years. In this study, Pearson correlation coefficient was used to compare the amount of anticipated average of monthly rainfall in series during the sampled years (2011- 2020) with the average amount of real and basic monthly precipitation in the last 10 years (2001-2010) to determine the accuracy of the anticipated model. Pearson correlation coefficient is obtained through equation 12 (Bayezid et al., 2012: 63):

$$r = \frac{(x-x-)(y-y-)}{\sqrt{(x-x-)^2(y-y-)^2}} \quad (12)$$

In order to evaluate drought monitoring in the upcoming years, SPI was used. SPI is an index that depends on the possibility of precipitation for any time and scale and is measurable for different time scales (1, 3, 6, 9, 12, and 24 months). This index can be an early warning for drought monitoring and help assess

its severity (Hejazizadeh & Javizadeh, 2010: 228). This method was proposed by McKee et al. (1993). Based on the investigations regarding different effects of shortage of precipitation on water resources, soil moisture and stream flow it can be calculated through equation 13 (Hejazizadeh & Javizadeh, 2007: 7):

$$SPI = \frac{P_i - \bar{P}}{S} \quad (13)$$

In that equation, P_i is the amount of precipitation in a given period, \bar{P} is the average of long-term precipitation in that period, and S is the standard deviation of precipitation. SPI values are obtained through equation (7) from long-term precipitation data for a period of time and they follow a normal distribution with an average of zero and a standard deviation of one. The numerical results make it possible to investigate humid and dry climates with the same method (Hejazizadeh & Javizadeh, 2010: 229). To calculate this statistic, gamma distribution is used to evaluate long-term data of precipitation. After the necessary calculations, determination of parameters related to SPI will be done. Gamma cumulative probability is measurable through equation (14):

$$G(X) = \frac{1}{B \Gamma(a)} \int_0^x t^{a-1} e^{-t/b} dt \quad (14)$$

In the above equation, a is the shape parameter, b is the scale parameter, x is the amount of precipitation, and $\Gamma(\cdot)$ is the gamma function. Shape and scale parameters can be estimated using maximum likelihood method and based on equations for each station and for each month of the year. So,

$$a = \frac{1}{4A} [1 + \sqrt{1 + 4A/3}] \quad b = X/a \quad (15)$$

Where, $A = \ln(X) = \ln(X)/n$ is the number of observations from precipitation. Variable x is the average of cumulative precipitation for a month during the sampled period. Because the gamma function is not defined for $x=0$ (precipitation is zero mm), distribution of rainfall may be zero. The total cumulative probability that includes also zero values can be obtained from equation (16):

$$H(X) = q + PG(X) \quad (16)$$

In this equation, q is the probability that precipitation levels would be zero and $p = 1 - q$. If M is the number of zero precipitations in time series of n , then q is obtained from equation (17):

$$q = m/n \quad (17)$$

After calculating the total cumulative probability ($H(X)$), standard normal random variable values and the

possible probability will be calculated by a probability with a mean of zero and a standard deviation of one. This value is the same as SPI. Equations from 18 to 21 present Z or SP from the values of ($H(X)$) (Hejazizadeh & Javizadeh, 2010: 229):

$$0.5 < Z = SPI = -[t - (c_0 + c_1 t + c_2 t^2 / 1 + d_1 t + d_2 t^2 + d_3 t^3)] \quad (18)$$

$$Z = SPI = + [t - (c_0 + c_1 t + c_2 t^2 / 1 + d_1 t + d_2 t^2 + d_3 t^3)] \quad (19)$$

$$t = \sqrt{\ln\left[\frac{1}{H(X)^2}\right]} \quad (20)$$

$$t = \sqrt{\ln\left[\frac{1}{(1 - H(X))^2}\right]} \quad (21)$$

In equations 18 to 21, c_0 c_1 c_2 d_1 d_2 & d_3 are constant rates, $H(X)$ is cumulative probability and $d_1 = 3.4327$ $d_2 = 0.1892$ $d_3 = 0.0033$ $c_0 = 2.5355$ $c_1 = 0.8028$ $c_2 = 0.03032$.

One advantage of this indicator is its flexibility compared to time scales and different statistics of SPI. It's also measurable and is graded in the range of +2 or more for acute wet, and in range of -2 for severe drought (Table 1). In this study, predicted monthly precipitation data from 2011 to 2020 in the station of Mashhad were simulated by using random patterns of time series. In order to monitor the severity of the drought, the data were entered into the SPI profile and were estimated by the use of algorithms in computing drought indices (DIP) software, drought severity, and frequency of different intensities in 6 and 12 months from 2011 to 2020.

RESULTS & DISCUSSION

Non-randomization of data was investigated using Ran test. This test rejected randomness of monthly precipitation data at 95% confidence interval in Mashhad station and indicated that these data are non-randomized and can be used to model and predict the future pattern. Using Mann-Kendall test, the trend of time series in monthly precipitation of Mashhad station was investigated. Fig. 2 shows that, the monthly precipitation data aren't enough for any trend. In order to evaluate the stability of the mean and variance statistical quality control charts were used. The results

Table 1. Drought classification based on SPI

Conditions	Extremely Wet	Very Wet	Moderately Wet	Normal	Moderately Dry	Severely Dry	Extremely dry
SPI rate	2 & more	1.5 to 1.99	1 to 1.49	0 to ±0.99	-1 to 1.49	-1.5 to -1.99	-2 & less

of statistical quality control chart (Fig. 3) indicate that monthly precipitation series in the average of (\bar{x}) is static, because the average curve has not deviated from its allowed range (between the UCL and LCL). In contrast, the series at variance is non-stationary.

An essential step in the analysis of time series is the stability of mean and variance. Given that the monthly precipitation time series of Mashhad station based on variance is non-stationary, in order to eliminate instability of variance and turn it into a stationary attribute, the power conversion of BOX-COX was used (equation 22). After fixing the variance (equation 22) and drawing on the diagram of BOX-COX (Fig. 4), using equation (23), converted monthly precipitation graph (static variance) was drawn (Fig. 5).

$$T(X_t) = x_t(\lambda) = x_t(\lambda) - 1/\lambda \tag{22}$$

where λ is between 2 and -2 and its value is calculated for the time series by trial and error in a way that the best value of λ makes Y_t distribution get closer to normal distribution. This conversion is used when the time-series changes are increasing or decreasing.

$$ntebi = \frac{1}{\sqrt[4]{x_t}} \tag{23}$$

As it can be observed in Fig. 5, the variance line is not outside of the boundaries in their control and is between the UCL and LCL lines with insignificant fluctuations and shows that the variance of monthly precipitation data of Mashhad has sufficient stability. According to time-series graph (Fig. 2), the series only has seasonality behavior of the monthly scale. For time-series analysis, seasonality behavior should also be removed from the time series. To do this, the series was differencing with lag of 12 and was called first order. So seasonality series with first order is differencing, and order D in the final model series of SARIMA (p, d, q) (P, D, Q) S, is equal to one (D=1). After using seasonality and non-seasonality differencing orders for initial series of monthly precipitation, in order to identify the model, ACF (Fig. 6) and PACF (Fig. 7) charts from differencing series were applied.

According to the graph of autocorrelation function (ACF), for a series of monthly precipitation, autocorrelation function values in all non-seasonality lag are zero and insignificant. Of course, insignificant autocorrelation in lag 1 of differencing series of ACF graph can be observed but can be ignored in selecting the appropriate model with fewer parameters. But in

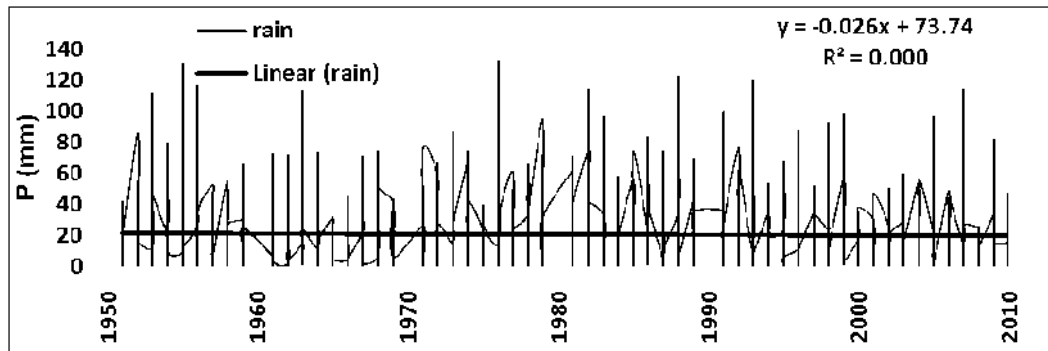


Fig. 2. Monthly rainfall time series of Mashhad station 2010-1951

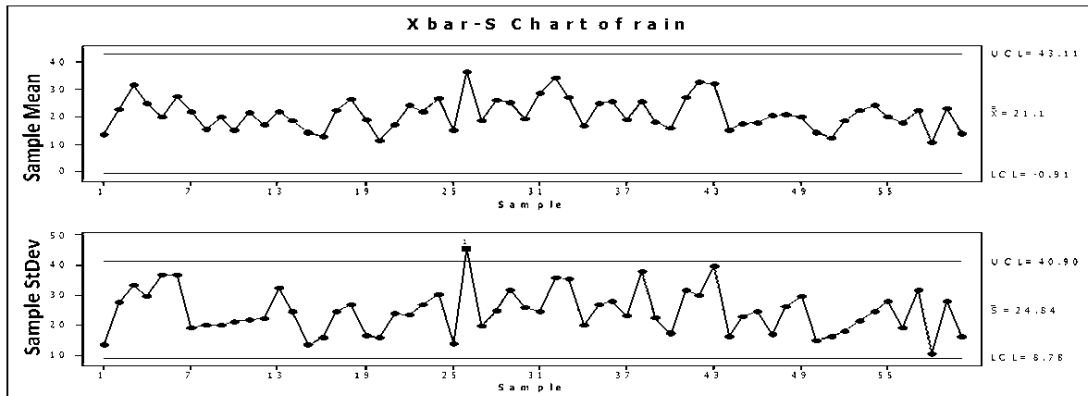


Fig. 3. Statistical quality control charts of mean (\bar{X}) and variance (s^2) for monthly precipitation of Mashhad station

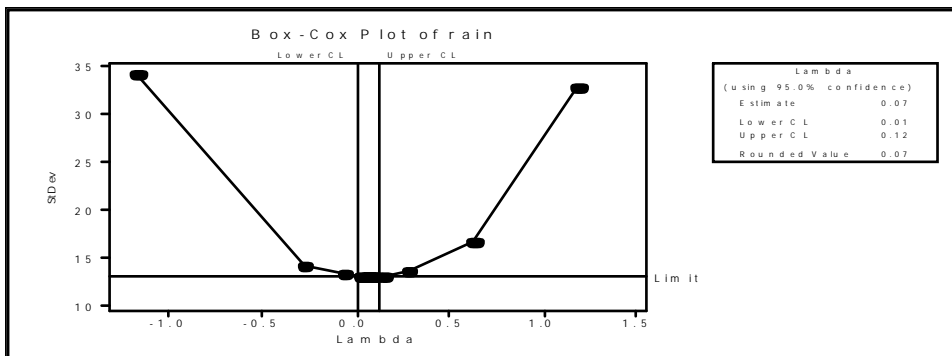


Fig. 4. BOX-COX of data

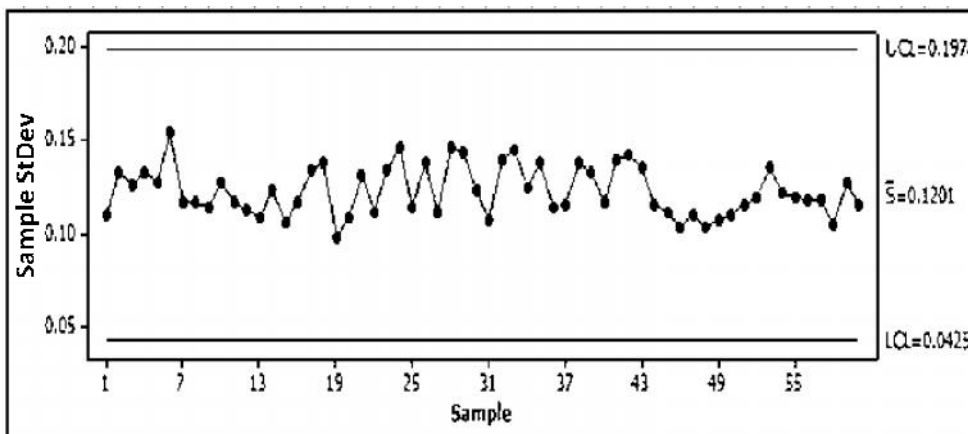


Fig. 5. Monthly rainfall data quality control charts after stabilization operations

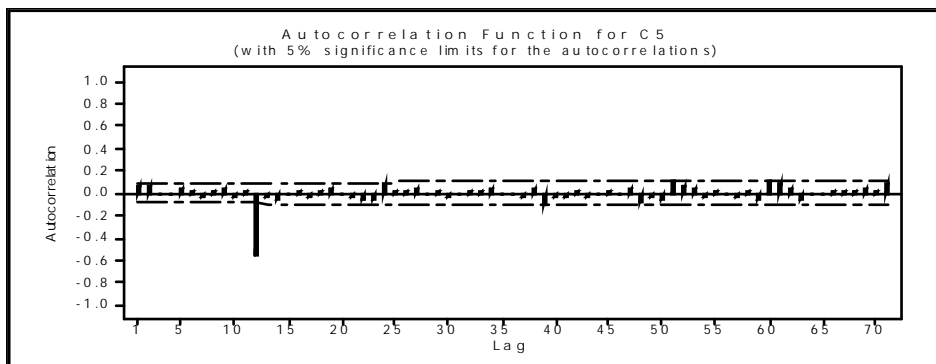


Fig. 6. Autocorrelation function graph

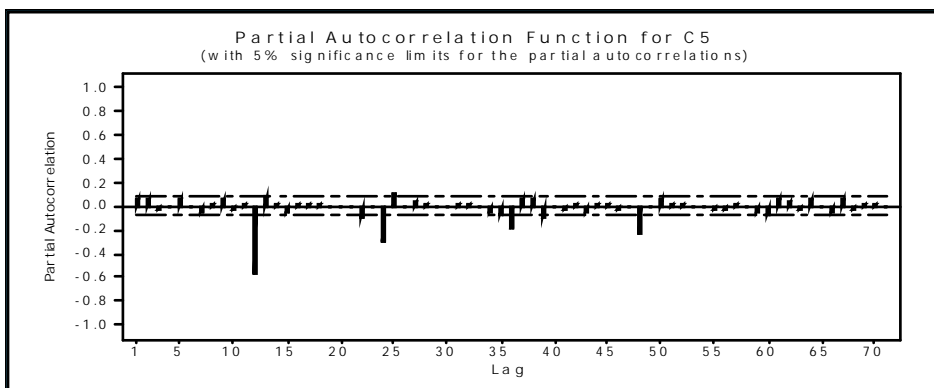


Fig. 7. Partial autocorrelation function graph

lag of 12 (the first lag of season) in ACF graph of differencing monthly precipitation series, a significant non-zero correlation equal to -0.449 can be observed which is out of the standardized range of autocorrelation function. Also according to PACF graph for differencing monthly precipitation series, it can be seen that the insignificant values of autocorrelation functions in seasonality lag (12, 24, 36 and 48) compared to autocorrelation function of ACF graph for differencing series with lower speed leans towards zero. As a result, the seasonal differential transformations with order 1 (D=1) seem good. On the other hand, the autocorrelation function graph indicates that the autocorrelation coefficient is significant in step 12. This indicates that the autocorrelation coefficient of seasonal periods stops after a step (step 12 non-seasonal data). However, the moving average model is a seasonal order (Q=1). Finally, within any 12-month period, a partial autocorrelation function is interrupted after step two. This represents the two-order autoregressive model (P=2). So, the appropriate model for the respected series is identified as SARIMA (2, 0, 1) (2, 1, 1). In other words, using the ACF and PACF, differencing series of monthly precipitation was considered as P=p=2 and Q=q=1.

Table 2. Results of the SARIMA model (2, 0, 1) (2, 1, 1) on time monthly precipitation series. The results of the model fitting on monthly precipitation time series are shown in Table 2. According to Table 2, (results fitting for SARIMA (2, 0, 1) (2, 1, 1) model on monthly

precipitation time series), the parameter of this model (λ) was calculated by T statistics and found to be 60.64 (p= .000) at 95% confidence interval. Furthermore, the null hypothesis or being zero constant term in model with statistics T is equal to -0.042 and is less than 2 and there is no need to incorporate the constant term in the model. The value of T is also greater than .05, so the null hypothesis cannot be rejected and it means the absence of a definite trend in the model. Khodagholi et al. (2014) investigated droughts in the upcoming years in Isfahan province using SARIMA model and showed that in the city of Isfahan, Meymeh, and Ardestan, ARIMA (1,0,0) (0,1,1) and in Nain, Fereydoun-Shahr, and Natanz, ARIMA (0,0,1) (0,0,1) had the highest correlation and being in line with the present study.

To examine the suitability of the fitted model and its comprehensive fitting, analysis of residuals in the fitted model was done by the help of graphs related to residuals. In addition, Port-Manto test was conducted. Results in Table 3 show that, the P-value for all delays is more than .05, so it can be claimed that residuals from fitted model are uncorrelated and the fitted model is a suitable model for monthly precipitation.

Then, the simulated average of monthly precipitation in Mashhad station in a 10-year period (2011-2020) was compared with the average of monthly real precipitation in a 10-year period (2001-2010). Using Pearson correlation coefficient, the correlation between

Table 2. Results of the SARIMA model (2, 0, 1) (2, 1, 1) on time monthly precipitation series

	Estimation	standard error	T Statistics	P-value
Coefficient ()	0.966	0.015	60.64	0.000
Constant	-0.042	0.052	-0.042	0.414

Table 3. Fitness of model and portmanteau test

Lag	12	24	36	48
Least Squares	6.2	15.7	26.4	42.4
DF	5	17	29	41
P- VALUE	0.410	0.604	0.545	0.285

Table 4. Simulated monthly precipitation (mm) for 2011 to 2020

Year	Jan	Feb	Mar	Apr	May	Jun	Jul	Agu	Sep	Oct	Nov	Dec
2011	36	30	80	30	22	2	2	2	2	2	23	23
2012	30	32	36	25	12	2	2	0	1	8	22	38
2013	27	14	59	20	23	3	1	2	0	1	22	26
2014	31	16	42	34	33	2	3	1	1	1	18	24
2015	27	34	71	37	31	3	1	1	2	1	30	18
2016	39	17	35	37	20	1	2	0	1	5	16	38
2017	26	22	79	33	32	4	2	3	0	1	21	11
2018	34	16	40	32	23	2	3	0	1	1	15	25
2019	24	37	92	24	25	5	1	1	3	1	20	20
2020	30	21	21	27	18	1	1	0	1	4	15	27

these two rainfall periods was estimated 96.5, which was significant at confidence interval of 95%. This high correlation level, can refer to high levels of simulated precipitation value in a 10-year period (2011-2020) using statistical model of seasonal-multiplicative ARIMA (2, 0, 1) (2, 1, 1)¹². Simulated precipitation amounts for the upcoming 10 years is offered in Table 4 and its relationship with the average of precipitation in 10 years (2001-2010) for better understanding is given in Fig. 8. According to Fig. 8, which compares the basic and future averages of precipitation, reduction of annual rainfall about 26mm in the next 10 years, is considered a major environmental hazard for the living things. Reduction of precipitation about 19mm in April will certainly have impacts on vegetation. This is a

warning for the environmental planners. In Fig. 8, the average rainfall between the base and coming years are compared. Rainfall in the upcoming years that predicted using this model will decrease in January, February, and April to October. A decrease in rainfall in the vegetation growth season in the next 10 years is considered a major environmental hazard.

After analyzing and simulating monthly precipitation in 2011-2020, the severity of the drought in the upcoming years in Mashhad station was examined using SPI (Table 5). The climatic conditions of Mashhad station are provided in terms of drought severity based on SPI on a scale of 6 months (short-term) and 12 months (long-term) in the upcoming years in the form of frequency and percentage (Table 5). Short-

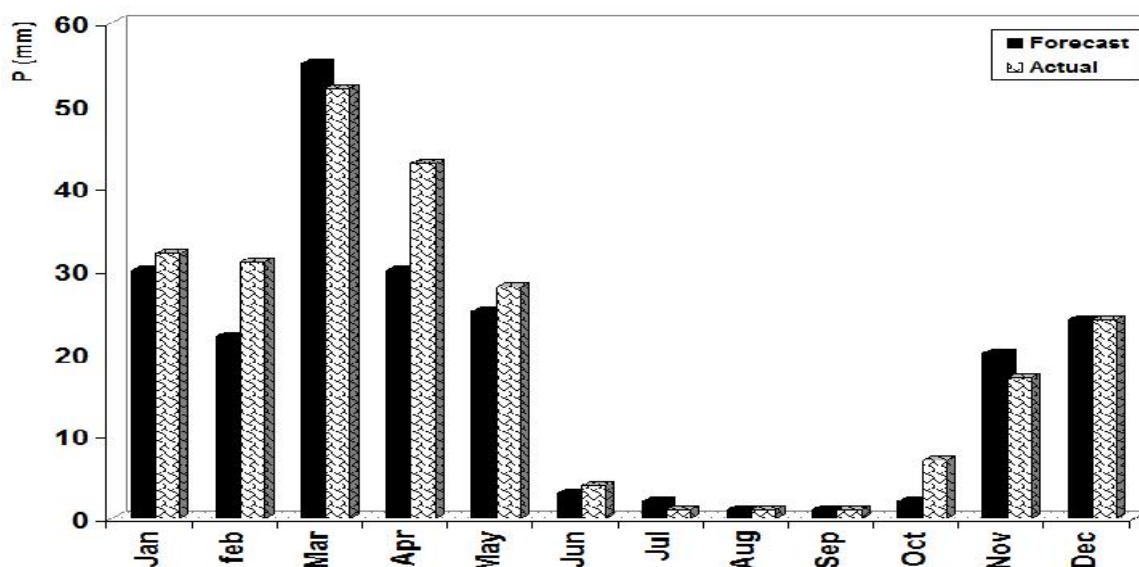


Fig. 8. Relationship between Simulated monthly rainfalls for 2020-2011 compared to the actual mean monthly rainfall for 2001-2010 in Mashhad station

Table 5. Frequency and percentage of occurrence of droughts in Mashhad station during the period 2020-2011 by SPI

Period Intensity	6 Month		12 Month	
	Frequency	Percentage	Frequency	Percentage
Extremely dry	0	0	4	3.6
Severely Dry	0	0	0	0
Severe Dry	6	5.2	0	0
Moderately Dry	15	13	15	13.7
Near Normal	64	55.6	55	50
Moderately Wet	25	21.7	31	28.4
Wet	1	0.8	0	0
very Wet	0	0	4	3.6
Extremely Wet	4	3.47	0	0
Total	115	100	109	100

term scale shows more fluctuations than the long-term scale; with the slightest change in precipitation, immediately it goes above zero, and if it is negative, it goes below zero. But long-term time scale reflects the drought better, and SPI values are related to floods, surface of water levels, and groundwater resources. According to Table 5, in the upcoming years in a 6-month scale, 18.2% of climate will be on drought conditions, 55.6% in normal condition, and 26% will have humid condition. But in a 12-month scale, 17.3% of climate will be on drought conditions, 50% in normal condition, and 32% will have humid condition.

CONCLUSIONS

According to the results predicted by the SARIMA model, it can be claimed that in Mashhad station, decline in the amount of precipitation is quite evident and it suggests that in the future we will have months and years with low precipitation. The difference and decline of 26mm in annual precipitation compared to the base period is indicative of the fact that in the coming years we should wait for lower precipitation in Mashhad plain. Climatic condition of Mashhad plain in the future years suggests the existence of drought condition about 18% in a 6-month scale and 17% in a 12-month time scale. According to the findings of recent studies as well as the current study, this can be considered a warning for the social life of humans and other living creatures in this plain. With regard to the prospect of decreased precipitation in this area, basic measures to deal with water shortages in the future for agriculture, industry, and drinking water consumption such as modifying irrigation systems and improving consumption patterns should be carried out by the environmental planners. Modification of cropping patterns in agriculture such as the using species with low water requirement, avoiding of development of industries with higher water consumption, managing current industries, planning and managing the reduction of water consumption through the development of a culture of water saving can be helpful strategies to deal with the effects of water shortage in the short terms and long term in Mashhad plain.

ACKNOWLEDGEMENT

The authors would like to thank Dr. Vali Mohammadi, University of Mohaghegh Ardabili, Ardabil, Iran, for his kind and valuable help in preparing the manuscript.

REFERENCES

Abdul-Aziz, A. R., Anokye, M., Kwame, A., Munyakazi, L. and Nsowah-Nuamah, N. N. N. (2013). Modeling and

forecasting rainfall pattern in Ghana as a seasonal ARIMA Process: The case of Ashanti region. *International Journal of Humanities and Social Science*, 3(3), 224-233.

Alivia Chowdhury, A. and Biswas, A. (2016). Development of a monthly rainfall prediction model using ARIMA techniques in Krishnanagar sub-division, Nadia District, West Bengal. *International journal of engineering studies and technical approach*, 2(2), 18-26.

Azarakhshi, M., Jalil, F., Eslah, M. and Sahabi, H. (2013). An Investigation on trends of annual and seasonal rainfall and temperature in different climatologically regions of Iran. *Journal of range and watershed management (Iranian journal of natural resources)*, 66 (1), 1-16.

Bari, S. H., Rahman, M. T., Hussain, M. M. and Ray, S. (2015). Forecasting monthly precipitation in Sylhet City using ARIMA model. *Civil and Environmental Research*, 7(1), 69-77.

Bazrafshan, O., Salajegheh, A., Bazrafshan, J., Mahdavi, M. and Fatehi Marj, A. (2015). Hydrological drought forecasting using ARIMA Models (Case study: Karkheh Basin). *Ecopersia*, 3, 1099-1117.

Bibi, U. M., Kaduk, J. and Balzter, H. (2014). Spatial-temporal variation and prediction of rainfall in Northeastern Nigeria. *Climate*, 2, 206-222. (doi: 10.3390/cli2030206).

Bayazidi, A., Oladi, B., Abbasi, N., Afrydon, K. (2012). *Statistical analysis with Minitab*. (Tehran: Abed Press).

Cancelliere, A. G., Mauro, B. and Bonaccorso, G. (2007). Drought forecasting using the standardized precipitation index. *Water Resource. Manage*, 21(5), 801-819.

Chun, K. P., Wheeler, H. and Onof, C. (2013). Prediction of the impact of climate change on drought: an evaluation of six UK catchments using two stochastic approaches. *Hydrological Processes*, 27, 1600-1614.

Djebbouai, S. and Souag-Gamane, D. (2016). Drought forecasting using neural networks, wavelet neural networks, and stochastic models: case of the Algerois basin in North Algeria. *Water Resources Management*, 30(7), 2445-2464.

Dodangeh, S., Abedi Koupai, J. and Gohar, S. A. (2012). Application of time series modeling to investigate future climatic parameters trend for water resources management purposes. *Journal of Water and Soil Science*, 16(59), 59-74.

Durdu, O. F. (2010). Application of linear stochastic models for drought forecasting in the Buyuk Menderes river basin, Western Turkey. *Stochastic Environmental Research and Risk Assessment*, 24(8), 1145-1162. (doi:10.1007/s00477-010-0366-3).

Eni, D. and Adeyeye, F.J. (2015). Seasonal ARIMA modeling and forecasting of rainfall in Warri Town, Nigeria. *Journal of Geoscience and Environment Protection*, 3, 91-98.

Etuk, E. H. and Mohamed, T. M. (2014). Time series analysis of monthly rainfall data for the Gadaref rainfall station, Sudan,

- by SARIMA methods. *International Journal of Scientific Research in Knowledge*, **2(7)**, 320-327.
- Fallah Ghalhari, G. A., Bayatani, F. and Fahiminezhad, E. (2015). Comparing the forecasting accuracy of the Box–Jenkins models in modeling seasonal precipitation (case study: the South of Kerman province, Iran). *Journal of Applied Environmental and Biological Sciences*, **5(12)**, 64-78.
- Ferrari, G. T. and Ozaki, V. (2014). Missing data imputation of climate datasets: Implications to modeling extreme drought events. *Revista Brasileira de Meteorologia*, **29**, 21–28.
- Ghahraman, N. and GharaKhany, A. (2011). Evaluation of random time series models for estimating evaporation pan (Case Study: Shiraz station). *Journal of Water Research in Agriculture*, **25 (1)**, 75-81.
- Golabi, M. R., Akhondali, A.M., Radmanesh, F. and Kashefipoor, M. (2014). Compare accurately predict of Box Jenkins models in seasonal rainfall modeling (Case study: selected stations in Khuzestan province). *Geographical Research Quarterly*, **29(114)**, 62-72.
- Han, P., Wang, P., Tian, M., Zhang, S., Liu, J. and Zhu, D. (2013). Application of the ARIMA models in drought forecasting using the standardized precipitation index. *Computer and Computing Technologies in Agriculture*, **392**, 352-358.
- Hejazizadeh, Z. and Javvizadeh, S. (2010). *An Introduction to drought and its parameters*. (Tehran: Samt Press).
- Ismaeilnejad, M. (2013). *Climate data processing*. (Birjand: Fekrebekr Press).
- Jayawardana, J., Dharshana Yapa, R. and Kumarathunge, D. (2016). Modeling extreme drought events in major cocount growing agro-ecological regions in Sri Lanka. *International Journal of Science and Research (IJSR)*, **5(19)**, 1249-1253.
- Karavitis, C. A., Vasilakou C. G., Tsesmelis D. E., Oikonomou P. D., Skondras N. A, Stamatakos, D., Fassouli, V. and Alexandris, S. (2015). Short-term drought forecasting combining stochastic and geo-statistical approaches. *European Water*, **49**, 43-63.
- Khodaghali, M., Sabouhi, R. and Eskandari, Z. (2014). Analysis of past trends of drought and it's predicted in future in Isfahan province. *Journal of Water and Soil Science*, **18 (67)**, 379-367.
- Mahgoub Mohamed, T. and Abd Allah Ibrahim, A. (2016). Time series analysis of Nyala rainfall using ARIMA method. *SUST Journal of Engineering and Computer Science (JECS)*, **17(1)**, 5-11.
- Matiur Rahman Molla, M. d., Shohel Rana, M. d., Sazzad Hossain, M. and Nuruzzman, S. M. (2016). Modelling monthly precipitation in Faridpur region of Bangladesh using ARIMA. *IOSR Journal of Environmental Science, Toxicology and Food Technology (IOSR-JESTFT)*, **10(6)**, 22-29.
- Meher, J. and Jha, R. (2013). Time-series analysis of monthly rainfall data for the Mahanadi River Basin, India. *Sciences in Cold and Arid Regions*, **5(1)**, 73–84.
- Mishra, A. K. and Singh, V. P. (2011). Drought modeling—A review. *Journal of Hydrology*, **403**, 157–175.
- Mohammadi, B. (2011). Trend analysis of annual rainfall over Iran. *Geography and Environmental Planning*, **43(3)**, 21-24.
- Mossad, A. and Ali-Alazba, A. (2015). Drought forecasting using stochastic models in a hyper-arid climate. *Atmosphere*, **6**, 410-430. (doi:10.3390/atmos6040410).
- Narayanan, P., Basistha, A., Sarkar, S. and Kamna, S. (2013). Trend analysis and ARIMA modelling of pre-monsoon rainfall data for western India. *Comptes Rendus Geoscience*, **345**, 22–27.
- Nirmala, M. and Sundaram, S. M. (2010). A Seasonal Arima Model for forecasting monthly rainfall in Tamilnadu. *National Journal on Advances in Building Sciences and Mechanics*, **1(2)**, 43–47.
- Ozger, M., Mishra, A. K. and Singh, V. P. (2011). Estimating palmer drought severity index using a wavelet fuzzy logic model based on meteorological variables. *International Journal of Climatology*, **31**, 2021–2032.
- Paulo, A. A., Rosa, R. D. and Pereira, L. S. (2012). Climate trends and behavior of drought indices based on precipitation and evapotranspiration in Portugal. *Natural Hazards and Earth System Sciences*, **12**, 1481–1491.
- Perez, G. J., Macapagal, V., Olivares, R., Macapagal, E. M. and Comiso, J. C. (2016). Forecasting and monitoring agricultural drought in the Philippines, *Remote Sensing and Spatial Information Sciences*. **XLI-B8**, 1263-2016. (doi:10.5194/isprsarchives).
- Shatanawi, K., Rahbeh, M. and Shatanawi, M. (2013). Characterizing, monitoring and forecasting of drought in Jordan River Basin. *Journal of Water Resource and Protection*, **5**, 1192-1202.
- Sheffield, J., Wood, E. F. and Roderick, M. L. (2012). Little change in global drought over the past 60 years. *Nature*, **491**, 435–438.
- Shirmohammadi, S. (2012). Investigation and modeling of temperature time series in Zanjan (1956-2005). *Geographical Research*, **27(4)**, 33-58.
- Sopipan, N. (2014). Forecasting rainfall in Thailand: A case study of Nakhon Ratchasima Province. *International Journal of Environmental, Chemical, Ecological, Geological and Geophysical Engineering*, **8(11)**, 777-781.
- Tian, M., Wang, P. and Khan, J. (2016). Drought forecasting with vegetation temperature condition index using ARIMA models in the Guanzhong plain. *Remote Sensing*, **8(690)**, 1-19.

Yu, M., Li, Q., Hayes, M.J., Svoboda, M. D. and Heim, R. R. (2014). Are droughts becoming more frequent or severe in China based on the standardized precipitation evapotranspiration index: 1951–2010?. *International Journal of Climatology*, **34**, 545–558.

Valipour, M. (2015). Long-term runoff study using SARIMA and ARIMA models in the United States. *Meteorological Applications*, **22**, 592–598.

Wang, H. R., Wang, C., Lin, X. and Kang, J. (2014). An improved ARIMA model for precipitation simulations. *Nonlinear Processes in Geophysics*, **21**, 1159–1168.